





Cite this: *RSC Adv.*, 2023, 13, 24755

Boosting functional properties of active-CMC films reinforced with agricultural residues-derived cellulose nanofibres†

Esther Rincón, ^{*a} Jorge De Haro-Niza,^{ab} Ramón Morcillo-Martín,^a Eduardo Espinosa ^a and Alejandro Rodríguez ^{*a}

The search for packaging alternatives that reduce the presence of non-biodegradable plastics in water is a focus of much research today. This fact, together with the increasing demand for active packaging capable of prolonging the shelf life of foodstuffs and the rise in the use of natural biopolymers such as cellulose, motivate the present work. This work evaluates CMC films loaded with gallic acid reinforced with (ligno)cellulose nanofibres from various agricultural residues as candidates for use in active food packaging. The first stage of the study involved the evaluation of different nanofibres as the reinforcing agent in CMC films. Increasing proportions of nanofibres (1, 3, 5 and 10% w/w) from horticultural residues (H) and nanofibres from vine shoots (V), containing residual lignin (LCNF) and without it (CNF), and obtained by mechanical (M) or chemical (T) pretreatment, were studied. The results of this first stage showed that the optimum reinforcement effect was obtained with 3% H-MCNF or 3% V-MCNF, where up to 391% and 286% improvement in tensile strength was achieved, respectively. These films offered slightly improved UV-light blocking ability (40–55% UV-barrier) and water vapor permeability (20–30% improvement) over CMC. Next, bioactive films were prepared by incorporating 5 and 10% wt of gallic acid (GA) over the optimised formulations. It was found that the joint addition of cellulose nanofibres and GA enhanced all functional properties of the films. Mechanical properties improved to 70%, WVP to 50% and UV light blocking ability to 70% due to the synergistic effect of nanofibres and GA. Finally, the bioactive films exhibited potent antioxidant activity, 60–70% in the DPPH assay and >99% in the ABTS assay and high antimicrobial capacity against *S. aureus*.

Received 14th June 2023

Accepted 31st July 2023

DOI: 10.1039/d3ra04003h

rsc.li/rsc-advances

Introduction

One of the biggest challenges facing society today is the reduction of plastics derived from fossil resources. Plastic waste has a drastic global impact on the environment. According to data reported by the European Commission in Directive (EU) 2019/904 on the reduction of the impact of certain plastic products on the environment, the 10 most common single-use plastic items on European beaches, together with fishing gear, account for 70% of all European Union (EU) marine litter.¹ Considering these problems and prioritizing the path towards sustainability described in the 2030 Agenda, the EU aims to reduce the volume and impact of certain plastic products on the environment. Many of the most common polluting plastic items

are related to food packaging, which is why the above-mentioned EU directive bans these products from entering the market. In this scenario, it becomes imminent to find new bio-based packaging solutions that prioritize the use of materials derived from renewable resources, preserving the necessary functionality with low environmental impact.² Finding effective packaging alternatives is the focus of much current research. Thus, natural biopolymers are increasingly being used as substitutes for petroleum derivatives worldwide as they provide an effective alternative to produce environmentally safe packaging materials that meet the market requirements.³

Cellulose is the natural biopolymer that has received increasing attention due to the desirable properties it imparts to materials incorporating it. Cellulose-based materials have better biodegradability compared to traditional packaging. For this reason, cellulose has gradually been introduced into the packaging industry. Cellulose-based materials meet market expectations satisfactorily. On the one hand, due to their successful performance in the various stages of the chain: protection, storage, transportation, market, *etc.* On the other hand, they satisfy the practical value, such as their convenient sale and environmental protection, cost reduction and sales

^aBioPrEn Group (RNM940), Chemical Engineering Department, Faculty of Science, Instituto Químico para la Energía y el Medioambiente (IQUEMA), Universidad de Córdoba, 14014, Córdoba, Spain. E-mail: a.rodriquez@uco.es

^bDepartment of Food Science and Technology, Faculty of Veterinary, Universidad de Córdoba, 14014, Córdoba, Spain

† Electronic supplementary information (ESI) available. See DOI: <https://doi.org/10.1039/d3ra04003h>



profit maximisation. That is why the development of all-cellulose based packaging materials are very promising.⁴

Carboxymethyl cellulose (CMC) is the most common polysaccharide derived from cellulose, which is the most abundant biopolymer on earth. CMC has already demonstrated its successful application in various fields including the food packaging industry.^{5,6} Characteristics such as its low cost, biodegradability and film-forming ability make it an ideal candidate for use in several packaging solutions such as edible coatings and films.⁷ Although being a good alternative to traditional plastics, natural biopolymers have certain inherent properties, such as low water resistance or poor mechanical properties, which make their application difficult. There are several ways to counteract these drawbacks, one of the most striking being the addition of nanomaterials. By adding these, the specific surface area of the matrix is increased, which could improve the barrier properties and mechanical strength of the nanocomposite films.⁸ One nanomaterial that is also applied is cellulose nanofibres (CNFs), another common cellulose derivative. This is a new type of polymer functional material that finds application in many different fields of interest, such as water decontamination,^{9,10} 3D bioprinting¹¹ and active food packaging.¹² In the case of the latter, CNFs are capable of improving the properties of polysaccharide films while maintaining their biodegradability. Due to their high aspect ratio, high tensile strength, high Young's modulus, high crystallinity and low coefficient of thermal expansion, CNFs are successfully employed as a reinforcing agent in polymeric matrices.^{13,14} The use of CNFs has the added advantage that they can be obtained from agricultural residues, a highly available and low-cost resource. In a previous investigation, the feasibility of two very abundant Spanish agricultural residues, horticultural residues (tomato, eggplant, and bell pepper mixture) and vine shoots residues, was explored to produce (ligno)cellulose nanofibres by high-pressure homogenisation, evaluating several pretreatments. As a result, several (ligno)cellulose nanofibres with suitable properties to be applied in the reinforcement of various materials were obtained.¹⁵

With the increasing demand for food safety, new packaging formulations must not only protect the food against the external environment while maintaining its quality, but also add new functionalities that help extend its shelf life. Thus, the food packaging industry is using antimicrobial and antioxidant agents as new packaging customisation technologies to prevent microbial contamination and food oxidation.^{16,17} One of the most used strategies is the addition of phenolic compounds since they have a powerful antioxidant and antimicrobial power.¹⁸ The addition of phenolic compounds reduces the use of synthetic antioxidants in the plastic, which limits the risk of toxicity due to migration phenomenon. Moreover, being present in the package, these phenolic compounds are released slowly and prolonged into the food, also contributing to reduce the addition of chemicals to the food. Polyphenols are natural compounds derived from plants with various health benefits including anti-inflammatory, anticancer, antimicrobial and antioxidant properties.¹⁹ Gallic acid (3,4,5-trihydroxybenzoic acid, GA) is one of these polyphenols with high antioxidant

capacity, due to both its redox properties and structural characteristics.²⁰ It is a molecule with 3 hydroxyl groups connected to a benzene ring as a weak polyprotic acid containing 4 acidic protons that can be transported to an acceptor base.²¹ Due to its properties, its use in packaging formulations is successful as it improves the oxidative and microbial status of foods in addition to the multiple benefits it brings to human health.^{22,23}

The present study aimed the integration of GA into CMC films reinforced with different (ligno)cellulose nanofibres obtained from horticultural residues and vine shoots. The reinforcing effect of the nanofibres on the CMC matrix, as well as the effect of the joint addition of the nanofibres and GA on the physical, functional, and bioactive properties of the composite films was investigated.

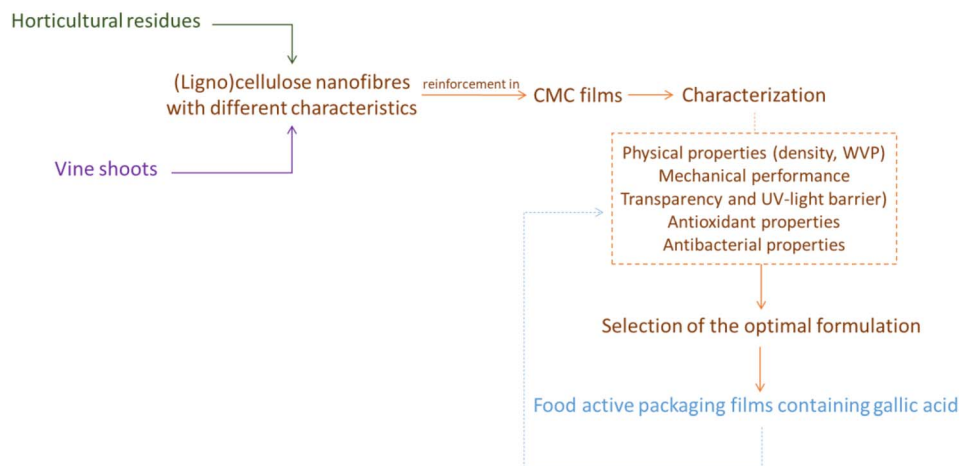
Experimental

Scheme 1 shows the experimental procedure followed during the development of this work. Briefly, different (ligno)cellulose nanofibres have been used as reinforcing agent in CMC films. Subsequently, these have been characterised to evaluate the influence of the various nanofibres and to find the optimum formulation in which the best reinforcing effect was achieved. This optimal formulation was used to prepare active films containing gallic acid as a bioactive ingredient, which were finally characterised.

Materials

The horticultural residues used in this study consisted of a mixture (in identical proportions) of bell pepper (*Capsicum annuum*), tomato (*Solanum lycopersicum*) and eggplant (*Solanum melongena*) supplied by Cooperativas Agrícolas de Almería (Andalucía, Spain). Vine shoots (*Vitis vinifera*) were supplied by Instituto de Investigación y Formación Agraria y Pesquera (IFAPA) from an organic farm in Cabra (Andalusia, Spain). Both raw materials were manually screened to remove undesired materials, dried at room temperature, and stored until use in plastic bags. Lignocellulose and cellulose nanofibres (LCNF and CNF, respectively) from horticultural residues (H) and vine shoots (V) were produced as reported in a previous investigation,¹⁵ by means of the two different pretreatments mentioned: chemical pretreatment based on a TEMPO-mediated oxidation (T) and the mechanical pretreatment through a mechanical beating (M). Briefly, the raw materials were subjected to a soda pulping process (100 °C, 150 min, 7% o.d.m. NaOH, liquid/solid ratio 10 : 1) to obtain unbleached cellulose pulp. T-pretreatment consisted of an oxidation reaction of this cellulose pulp with 5 mmol NaClO/g fibre and subsequent addition of 0.5 M NaOH to keep the pH stable at 10.2. Once the reaction time (2 h) had elapsed, the reaction was stopped by the addition of ethanol, the pretreated pulp was filtered, and a 1.5% suspension was prepared and subjected to a high-pressure homogenisation (HPH) process to obtain the LCNF. In the case of M-pretreatment, a 1.5% suspension of the cellulose pulp was prepared and subjected to a mechanical refining process up to a Shopper-Riegler degree (°SR) of 90. In the case of obtaining





Scheme 1 Experimental procedure carried out during this study.

Table 1 Cellulose and lignin content of the different cellulose pulps used in this work

Raw material	Type	Cellulose (%)	Lignin (%)
Horticultural residues	Unbleached	50.5	16.0
	Bleached	64.4	7.3
Vine shoots	Unbleached	51.9	14.2
	Bleached	67.2	6.4

CNF, the starting cellulose pulp was bleached with NaClO_2 prior to the pretreatments. The cellulose and lignin content of the different cellulose pulps used in this work is shown in Table 1, according to the determination reported in a previous work.¹⁵ By this way, (L)CNF used in this work were named according to the raw material from which they were derived, and the pretreatment used, thus considering eight types of nanofibres: H-MLCNF, H-MCNF, V-MLCNF, V-MCNF, H-TLCNF, H-TCNF, V-TLCNF, and V-TCNF.

The characteristics usually studied in (L)CNFs (cation demand, carboxyl content, and specific surface area) of all the nanofibres used in this study have been reported in a previous work.¹⁵ Diameter and length were estimated using a theoretical model based on the measurement of intrinsic viscosity correlated with the degree of polymerisation. For the present study, these data have been corroborated by transmission electron microscopy (TEM) observation, showing similar diameters to that previously estimated (Fig. S1†).

Carboxymethylcellulose sodium salt (medium viscosity, 0.9 substitution, average molecular weight 70 000), gallic acid (anhydrous), 2,2-diphenyl-1-picrylhydrazyl (DPPH, 394.32 g mol⁻¹) and 2,2'-azino-bis(3-ethylbenzothiazoline-6-sulfonic acid) diammonium salt (ABTS, 548.98 g mol⁻¹) were provided from Sigma-Aldrich; glycerol (pure, pharma grade) was provided from PanReac AppliChem ITW Reagents. Methanol (>99.8% purity) and ethanol (96% purity) were supplied by Labkem.

Films production

Films with a grammage of 35 g m⁻² were prepared by the solvent casting method. Firstly, a 2% (w/w) CMC stock solution containing 30% (w/w) glycerol was prepared under mechanical stirring for 3 h at 60 °C. Then, the respective amount of the stock solution was diluted until a final volume of 100 mL, cast in a square Petri dish of 12 cm² and dried in a conditioned room at 25 °C and 50% HR obtaining the blank film. The blended films, containing CMC and (L)CNF, were prepared starting from the homogenisation of the appropriate amount of (L)CNF in distilled water using a high-shear homogeniser (IKA T18 digital Ultra Turrax) to obtain final (L)CNF concentrations of 1, 3, 5, and 10% (w/w). Then, these (L)CNF solutions were mixed with the CMC:Gly stock solution at a final concentration and made up to 100 mL with distilled water. These mixtures were magnetically stirred for 3 h to allow the cross-linking reaction between the polymers. The casting and drying of the films were in an analogous manner that for the CMC film samples. The resulting films were labelled according to the proportion and type of (L)CNF included in the formulation.

Active films containing GA were prepared in an analogous manner. A solution of GA in distilled water (10 mg mL⁻¹) was prepared and added to the mixture of CMC and (L)CNF during the stirring step. The volume of dilution added was the volume necessary to reach a concentration of 5 or 10% wt GA in the final films.

Film properties evaluation

Physical properties. The density of the films was determined in triplicate by measuring their weight, area, and thickness (Digital Micrometer IP65-293, Digimatic, Mitutoyo, Neuss, Germany with a sensitivity of 1 µm).

Water vapor permeability (WVP) was determined by the Desiccant Method according to ASTM E96/E96M-10 standard test.²⁴ These measurements were performed in TQC Sheen Permeability Cups (Industrial Physics, Boston, MA, USA) of an anodized aluminum with 10 cm² surface area containing CaCl_2 .



as desiccant material. The tests were carried out in triplicate for 24 h during which the capsules were stored in a climatic chamber ICHeco (Mettler, Büchenbach, Germany) at 25 °C and 50% relative humidity. WVP was calculated following eqn (1) from the data of water vapor transmission rate (WVTR) obtained from eqn (2).

$$\text{WVP} = \frac{\text{WVTR}}{\Delta p} = \frac{\text{WVTR}}{S(R_1 - R_2)} \quad (1)$$

where, Δp is the vapor pressure difference (Hg), S is the saturation vapor pressure at test temperature (Hg), and R_1 and R_2 are the relative humidities at the source and at the vapor sink, respectively, expressed as a fraction.

$$\text{WVTR} = \frac{G}{tA} \quad (2)$$

where, G is the weight change (g), t the time during which G occurred (h) and A is the test area (cup mouth area, ft²).

Mechanical properties. Mechanical performance of the prepared films was determined in terms of tensile strength and Young's modulus values according to ASTM D882 standard test.²⁵ Analyses were performed in film specimens of 10 cm gauge length and 1.5 cm wide using a Universal Testing Machine model LF Plus Lloyd Instrument AMETEK Measurement & Calibration Technologies Division (Largo, FL, USA) of 1 kN load cell. Tests were performed with an initial grip separation of 7 cm and the crosshead speed was set at 10 mm min⁻¹. Results were expressed as an average of ten samples for each type of film.

Optical properties. Optical properties in terms of light transmittance and UV-barrier capacity were determined by measuring the light transmittance of the films at 660 and 280 nm, respectively, using a Jenway 7315 Advanced UV/Visible Spectrophotometer (Stone, Staffordshire, UK).²⁶

Morphology observation. The surface morphology of the films was assessed with Scanning Electron Microscopy (SEM). The microscope was a field emission scanning electron microscope JEOL JSM 7800F. Film specimens of 10 × 10 mm were coated using conductive gold sputter at 10 kV.

Antioxidant properties. DPPH (2,2-diphenyl-1-picrylhydrazyl radical) and ABTS [2,2'-azino-bis(3-ethylbenzothiazoline-6-sulfonic acid)] methods were used to evaluate the antioxidant activity of the bioactive films.²⁷ For the DPPH analysis of the bioactive films, 50 mg of film sample was placed in 10 mL of DPPH solution (0.2 mM DPPH in methanol) and incubated at room temperature for 30 min in darkness. Then, the absorbance of the solution was measured at 517 nm and the radical scavenging activity (RSA) was calculated following eqn (3).

$$\text{RSA (\%)} = \frac{\text{ABS}_{\text{control}} - \text{ABS}_{\text{sample}}}{\text{ABS}_{\text{control}}} \times 100 \quad (3)$$

where, $\text{ABS}_{\text{control}}$ is the absorbance of the DPPH starting solution (0.2 mM DPPH in methanol) and $\text{ABS}_{\text{sample}}$ is the absorbance of the DPPH solution in contact with the film piece for 30 min in the dark.

For the ABTS analysis of the film samples, an ABTS solution (7 mM ABTS in 2.45 mL K₂S₂O₈) was prepared and left to stand

in the dark for 14 h prior to use. The absorbance of the ABTS solution was adjusted to 0.70 ± 0.02 at 734 nm using a hydro-alcoholic mixture (ethanol:water, 1:1). Then, 50 mg of film samples was placed in 10 mL of ABTS solution and incubated at room temperature for 6 min in darkness. Lastly, the absorbance of the solution was measured at 734 nm, and the antioxidant power (AOP) was calculated following eqn (3).

Antibacterial properties. The agar disk diffusion method was used to measure the antimicrobial activity of the bioactive films. The inhibitory effect on the growth of two important foodborne pathogenic bacteria, *S. aureus* and *E. coli* was studied. To perform the test, the films were cut into squares of 15 × 15 mm and sterilised by exposing them to UV-light for 20 min. Lawns of the target bacteria were performed from a standardised suspension (1×10^8 UFC mL⁻¹ 0.1–0.08 absorbance at 625 nm) in the surface of Mueller Hilton agar Petri dishes. The sterilised films were placed upon the lawns and the Petri dishes (9 cm ϕ) were incubated at 37 °C for 24 h. After 24 h the diameters of the inhibition zones were measured, and the antimicrobial activity was calculated following eqn (4).

$$\text{Antimicrobial activity (mm)} = D - d \quad (4)$$

where D is the diameter of the inhibition zone and d , the film dimension.

Statistical analysis

The experimental results were expressed as the average \pm standard deviation. Analysis of variance (ANOVA) followed by the Duncan post hoc test was performed. Different letters show significant differences ($p \leq 0.05$).

Results and discussion

Nanocellulose inclusion effect in CMC films

In the first stage of the study, CMC films were reinforced with increasing amounts (1, 3, 5, and 10% wt) of the eight different (ligno)cellulose nanofibre types previously mentioned. In this way, it would be possible to evaluate not only whether nanofibres work properly as a reinforcing agent for biopolymers such as CMC, but also the influence of the raw material, the pretreatment process applied to obtain them as well as the presence of residual lignin in them.

Density and barrier ability against water vapor. Physical properties of the prepared films comprising density and WVP are displayed in Fig. 1. The density was strongly influenced by the proportion and type of nanofibres included in the films. In general, the density of the films decreased upon incorporation of the reinforcing agent as a result of strong adhesion between the polymer chains. This reinforcement was more noticeable when 3% wt of nanofibres were included in the structure, with no significant changes when higher proportions were included. The raw material from which the nanofibres were obtained did not make a great difference, but the pretreatment applied to obtain them, and the presence of residual lignin did. Thus, the use of H-MLCNF, H-TLCNF, V-MLCNF and V-TLCNF generally resulted in a more prominent decrease in density than when



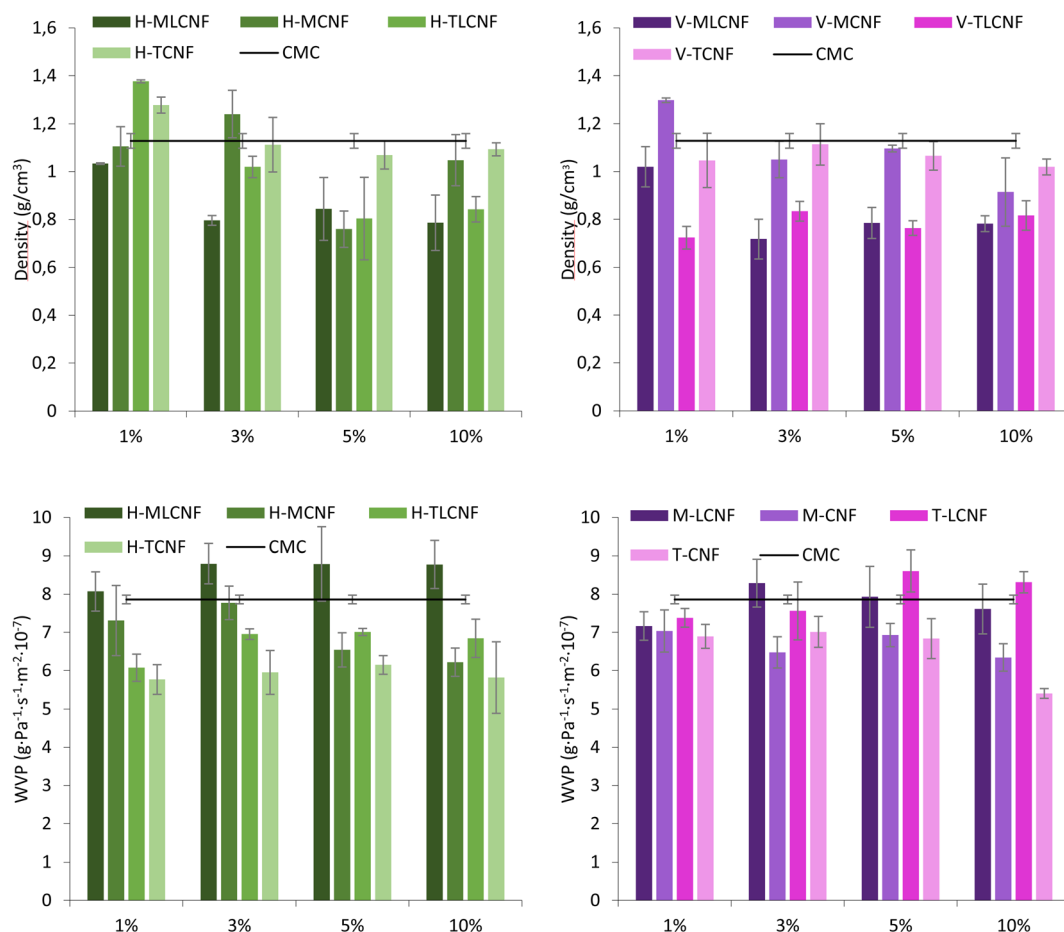


Fig. 1 Density and WVP of (L)CNF-reinforced CMC films.

lignin-free nanofibres were used. The absence of lignin in CNF leads to stronger self-association between the nanofibres resulting in higher densities.¹² On the other hand, this decrease in density was more prominent in the case of using mechanically pretreated nanofibres. In general, lignin free-nanofibres pretreated by TEMPO-mediated oxidation present higher proportion of $-OH$ groups available for interaction with other molecules. This was demonstrated in a previous study where H-TCNF and V-TCNF presented the highest cationic demands (1043.54 and 1227.91 $\mu\text{eq. g}^{-1}$, respectively) and specific surface areas (436 and 516 $\text{m}^2 \text{g}^{-1}$, respectively) of all nanofibre types studied.¹⁵ These facts translate into a higher interaction with CMC resulting in films of higher densities.

The WVP results of the films showed that the inclusion of nanofibres in their structure increased the water vapor resistance, in agreement with studies reported in literature.³ However, for this property, significant differences were found between raw materials. For horticultural-nanofibres, this decrease in WVP was observed for H-MCNF, H-TLCNF and H-TCNF. Considering the characteristics of these nanofibres, it seems that cationic demands, carboxyl contents and specific surface areas above 600 $\mu\text{eq. g}^{-1}$, 70 $\mu\text{eq. g}^{-1}$ and 250 $\text{m}^2 \text{g}^{-1}$, respectively, are required to achieve the desired effect.¹⁵ Furthermore, in the case of vine shoots-nanofibres, this

improvement in WVP is achieved only if the nanofibres do not contain residual lignin. All these effects were again observed with the incorporation of 3% wt of nanofibres in the films, the results not varying significantly when higher proportions were included. Two hypotheses can explain the results found for the physical properties evaluated. On the one hand, a high specific surface area and proportion of $-OH$ groups by the nanofibres are needed to interact with the CMC correctly and form homogeneous films. Although the presence of lignin can be beneficial for other active properties, in this case, lignin seems to inhibit the desired effects by causing a disruption in the structure of the films which decreases the film density and increases the WVP. On the other hand, it has been reported that the higher WVP of CNF-containing films is related to the crystalline structure of the films, which is able to hinder water vapor diffusion. Kim *et al.*, reported that an increase in the crystallinity indices of the films implies a decrease in the WVP of the films.²⁸ Furthermore, other authors showed that the crystallinity index of the films increases as the crystallinity index of the CNFs decreases.^{29,30} The results obtained in this study support this hypothesis, since according to previous studies, H-MLCNF presents the highest crystallinity index of all the nanofibres involved in this work.²⁹ This would result in films with lower crystallinity indexes and, therefore, lower WVP.



Mechanical response of the composite films. Mechanical properties of the (L)CNF-reinforced CMC films in terms of tensile strength (TS) and Young's modulus (YM) are displayed in Fig. 2. As clearly observed, the reinforcing effect of nanofibres on CMC films was successfully achieved. In general terms, this effect was achieved with 3% wt of nanofibres with no significant increases with higher proportion of nanofibres in the material. The use of horticultural-nanofibres resulted in slightly higher values than vine shoots-nanofibres. Thus, for example, films reinforced with 3% H-MCNF showed a 391% improvement in TS over the CMC film, compared to the 283% improvement achieved with 3% V-MCNF films. The elastic modulus followed the same trend with higher values when using horticultural-nanofibres. In addition, clear differences were observed between the types of the nanofibres used. Thus, the lowest TS values in the case of horticultural-nanofibres were obtained when H-MLCNF and H-TLCNF were used. It seems that the presence of residual lignin in these fibres is related to this lower TS. TEMPO-mediated oxidation applied as a pretreatment to obtain H-TLCNF modifies the C6 carboxyl groups of cellulose, however, when lignin is present in the reaction medium it competes in the use of the reagents. This is why, in the case of H-TLCNF, the minor reinforcing effect observed is more moderate than in the case of H-MLCNF (Fig. S2†). Several

authors have reported that the use of LCNF in the preparation of polymeric films results in high mechanical reinforcement given the presence of residual lignin. This lignin would act as a gap filler in the structure during film formation, acting as an adhesive between the fibres and giving a plasticizing effect.³¹ As shown, the films prepared in this work with horticultural-nanofibres did not support this hypothesis since the highest results were obtained in the case of lignin-free nanofibres. This is due to the higher specific surface area presented by H-MCNF and H-TCNF (298 and 426 m² g⁻¹, respectively) compared to H-MLCNF and H-TLCNF (129 and 262 m² g⁻¹, respectively), determined in a previous study.¹⁵ As reported by several authors, nanofibres intertwine in a three-dimensional network more easily when lignin is not present, resulting in stronger adhesion and crosslinking between the molecules resulting in a higher reinforcement effect.^{12,32} In the case of using vine shoots-nanofibres, clear differences were also found between the type of pretreatment used to obtain them. Thus, the highest TS values were achieved when V-MCNF were used. Again, the morphology of these nanofibres underlies the behaviour found. Considering the length and diameter of vine shoots-nanofibres reported in a previous investigation,¹⁵ the aspect ratio is obtained by simply dividing these two values. Thus, the aspect ratios for the vine shoots-nanofibres were 101, 434, 137, and 151

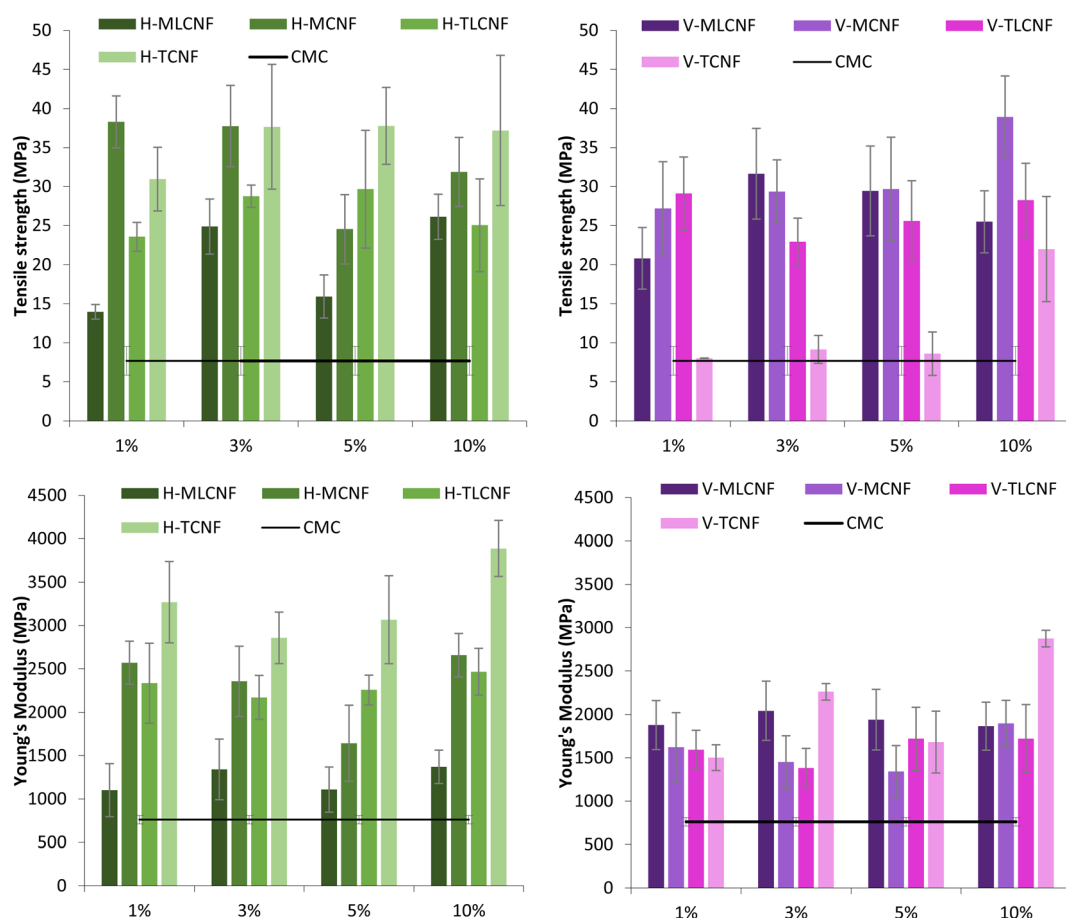


Fig. 2 Mechanical properties of CMC/nanofibres-based films.



for V-MLCNF, V-MCNF, V-TCNF and V-TLCNF, respectively. Therefore, a higher aspect ratio seems to be directly related to an optimal reinforcement of CMC films. However, the values obtained for YM did not follow this trend, indicating that although the reinforcing capacity of the materials using V-MCNF increased, they became slightly stiffer compared to the other types of vine shoots-nanofibres used (Fig. S3†). In all cases, the elastic modulus increased significantly compared to CMC films. Other authors have reported similar behaviours when including nanoparticles in polymer films, attributing it to a desirable interaction between the matrix components.⁷ Furthermore, it is worth mentioning that the values achieved for TS and YM for the optimal CMC and (L)CNF formulations in this work are very close to the values reported in literature for thermoplastic-based films such as PLA. Auras *et al.*, reported TS and YM of 44–66 MPa and 3750–4190 MPa, respectively, for films formed by various types of PLA.³³ Polylactide polymers have been used in recent years for the replacement of traditional synthetic packaging materials. The fact that the mechanical properties of CMC have been improved by incorporating nanofibres to values close to PLA suggests that it could be used as a new source of bio-based polymer in the packaging industry.

Transparency and UV-light blocking capacity. The transparency (% T_{660}) and UV-light blocking ability of the films are shown in Fig. 3. As the light transmittance values show, the films become relatively opaque with increasing nanofibre content, decreasing from 87% light transmittance for pure CMC to 51.7–74% for the maximum proportion of horticultural-nanofibres and 51.2–64.8% for the maximum proportion of vine shoots-nanofibres. Overall, TEMPO-oxidised nanofibres reduced the light transmittance of the films to a lesser extent compared to those nanofibres subjected to mechanical pretreatment, revealing better light scattering. In addition, those films reinforced with LCNF showed higher opacity than those reinforced with CNF, as a result of the presence of lignin-containing fibres. These differences in light transmittance between the different types of nanofibres are attributed to the morphology of the nanofibres, mainly diameter and length.²⁸ Shorter, smaller diameter fibres will allow higher light transmittance than long, wide fibres. As the transparency of the films decreased with nanofibre content, the UV light blocking ability increased. Thus, it went from a 13% UV-light barrier in CMC films to 46–51% for those films with higher proportions of nanofibres. Very clear differences were again observed between the use of LCNF and CNF. As previously reported, the chemical composition of lignin with a high content of phenolic

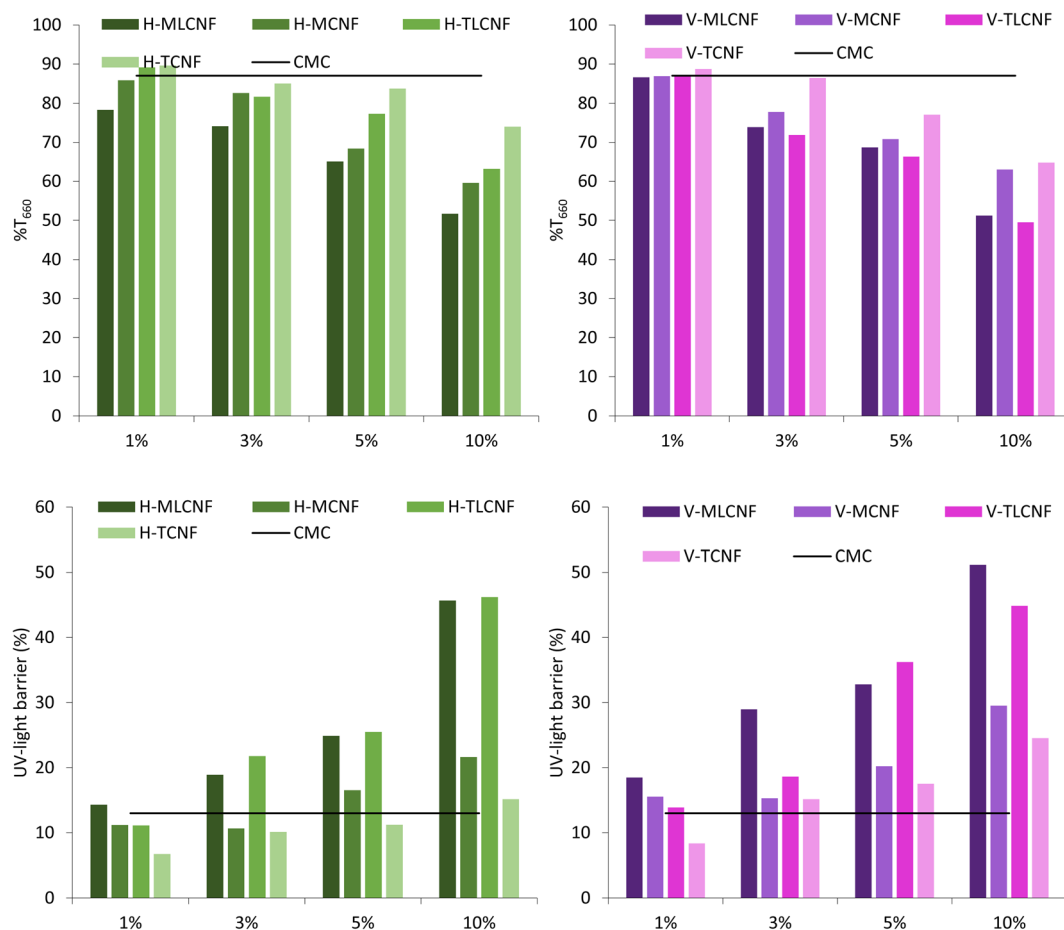


Fig. 3 Optical properties of CMC/nanofibres-based films.

compounds and conjugated carboxyl groups increases UV-light absorption.³¹ This also underlies the fact that the UV-light barrier capacity is higher in the case of mechanically pre-treated nanofibres. Previously, it has been mentioned that TEMPO-mediated oxidation also attacks lignin so it would be less reactive in those nanofibres to interact with light radicals. The results obtained for this barrier capability were promising about the possibilities of nanofibre-reinforced CMC films for the preparation of packaging materials. By incorporating the nanofibres into the matrix, values were achieved that exceed the currently employed PLA films, whose barrier capacity to UV-light is around 23%.³⁴

Surface morphology of the composite films. As a last step in the evaluation of the CMC films reinforced with the different nanofibres, their surface morphology was studied (Fig. 4). The control film (CMC) was observed to have a smooth, continuous and homogeneous surface. Some cracks were observed but they are attributed to the drying process and preparation of the samples. It could be stated that the mixing between CMC and glycerol was adequate. It was observed that the inclusion of nanofibres at high proportions in the film resulted in an increase in film roughness. At low nanofibre ratios (3% H-MCNF and 3% V-MCNF, Fig. 4b and d, respectively), it was observed that the roughness was practically unchanged with respect to the CMC film. Well dispersed bundles of nanofibres

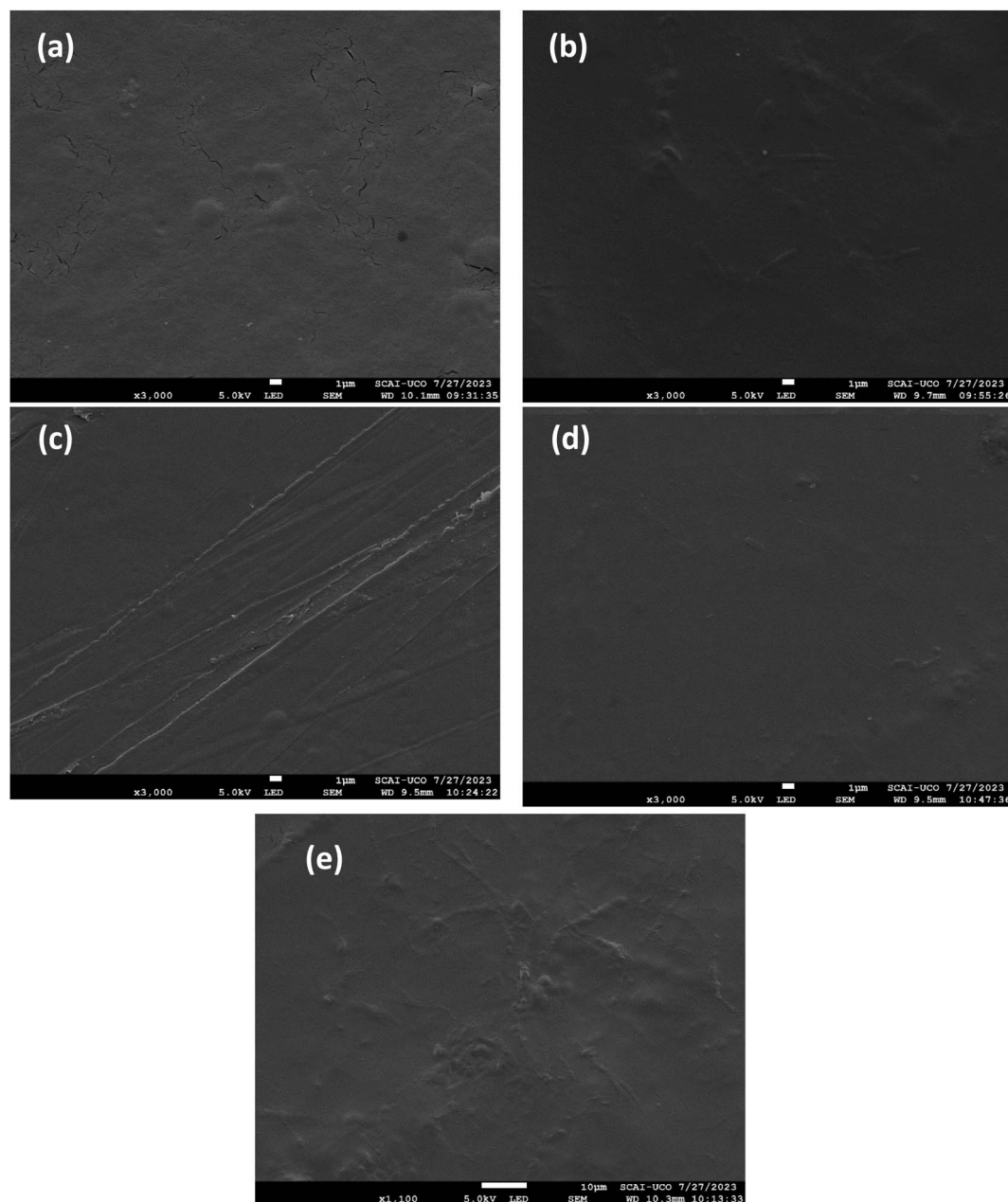


Fig. 4 SEM images of (a) CMC, (b) 3% H-MCNF, (c) 10% H-MCNF, (d) 3% V-MCNF and (e) 10% V-MCNF films.



were observed embedded in the films, while increasing the proportion to 10% nanofibres resulted into rougher and more irregular surfaces due to the agglomeration of the nanofibres in the matrix. Similar results have been reported by other authors who demonstrated that high proportions of nanofibres in starch films caused a selective agglomeration of the nanofibres in the material leading to inhomogeneity of the nanofibres.³⁵ This higher homogeneity of films with 3% nanofibres underlies the higher reinforcement effect previously reported. No significant differences were found between the raw materials used.

Bioactive films through the incorporation of gallic acid

Once the evaluation of the different nanofibres at increasing ratios was completed, bioactive films incorporating GA as the active agent were formulated. For these bioactive films, 3% H-MCNF and 3% V-MCNF were taken as the optimal reinforced formulation. As previously discussed, this proportion of nanofibres in the materials was sufficient to achieve the desired reinforcing effect, since no large variations were found when including more nanofibres. In addition, nanofibres obtained by mechanical pretreatment were chosen instead of those obtained by chemical pretreatment. This fact is not only supported by the results obtained, but from the point of view of economic and environmental feasibility, the use of mechanical pretreatment is preferable. Recent studies comparing the life cycle assessment of the different pretreatment routes for obtaining nanofibres have reported that the mechanical route has the lowest environmental impact, as well as milder contribution to climate change, acidification, eutrophication, and other indicators.³⁶ Bioactive films with two different percentage of GA were prepared (5 and 10% wt).

Prior to the evaluation of their bioactivity, the bioactive films were evaluated according to the same parameters previously measured. The incorporation of this active compound could not only increase their bioactivity, but also alter the physical, mechanical, and optical properties of the polymer matrix. Physical, mechanical, and optical properties of the bioactive films are summarised in Table 2.

In general, the incorporation of GA in films resulted in an improvement in all the properties evaluated. Thus, the WVP decreased considerably with the inclusion of this active compound. The addition of GA in the formulation resulted in an improvement of more than 50% in the WVP. No significant

differences were found between increasing amounts of GA. The incorporation of active compounds in polymeric matrices such as GA affect the gas permeation process due to a change in the diffusion process. Other authors have reported these same trends when incorporating active ingredients such as quercetin or alizarin into polymeric matrices.^{16,37} WVP is one of the most important properties of food packaging since it allows estimating the water vapor transfer between the packaged food and the surrounding environment. The presence of nanoparticles, in this case CNF, and GA occupies the voids in the CMC-macromolecular network decreasing the WVP.³⁸

The incorporation of GA into the formulation positively affected the mechanical behaviour of the bioactive films, as displayed in the strain–stress curves of the bioactive films (Fig. S4†). Specifically, the addition of GA resulted in a 25–30% improvement in TS for H-MCNF-reinforced films and a 50–70% improvement for V-MCNF films. Interestingly, increasing proportions of GA did not yield significant differences, suggesting that even as little as 5% wt of GA can achieve optimal improvement. In addition, the films became more elastic as GA was added in the formulation. This effect was again most prominent for the V-MCNF reinforced films where the YM of the films was increased to 94%. These differences between nanofibre matrices are explained by previous results where the reinforcing effect of V-MCNF was lower than that of H-MCNF due to a lower specific surface area. This is counteracted by adding GA in the formulation. This enhanced mechanical response is due to the formation of intermolecular interactions between the polyhydroxy groups of GA and the hydrophilic groups of CMC that form a compatible complex between the two compounds.¹⁶ Similar results have been reported for chitosan and gelatin films incorporating a relatively low dose of GA. The incorporation of GA enhances the structural bonds in the polymer network.^{39,40}

Optical properties were also affected by the presence of GA. Thus, the opacity of the films increased slightly with the lower dose of GA while they became relatively more transparent with the higher amount (% T_{660} increased from 77.8% for 3% V-MCNF to 86.3% for V-10% GA). A correct dosage of GA seems not only to improve the structural properties of CMC films but also to promote a correct dispersion between the matrix components, hence the transparency slightly increased with respect to the blank. However, the best result obtained in this

Table 2 Characteristics of bioactive films in terms of physical, mechanical, and optical properties^a

Film	Density (g cm ⁻³)	WVP [†] (g Pa ⁻¹ s ⁻¹ m ⁻² 10 ⁻⁷)	TS ^{††} (MPa)	YM ^{†††} (MPa)	% T_{660}	UV-light barrier (%)
3% H-MCNF	1.24 ± 0.10 ^a	7.77 ± 0.44 ^a	37.75 ± 5.20 ^a	2356.56 ± 404.22 ^a	82.6	10.65
H-5% GA	1.08 ± 0.10 ^b	4.53 ± 0.19 ^b	48.74 ± 12.8 ^b	2701.43 ± 143.03 ^a	78.3	75.10
H-10% GA	1.03 ± 0.05 ^b	3.56 ± 0.40 ^c	46.82 ± 4.94 ^b	2769.79 ± 362.64 ^a	82.9	74.55
3% V-MCNF	1.05 ± 0.08 ^b	6.47 ± 0.41 ^d	29.36 ± 4.07 ^a	1450.80 ± 303.88 ^b	77.8	15.30
V-5% GA	1.07 ± 0.01 ^b	4.62 ± 0.10 ^b	49.31 ± 9.19 ^b	2807.07 ± 436.69 ^a	72.4	76.24
V-10% GA	1.07 ± 0.10 ^b	3.55 ± 0.19 ^c	44.38 ± 7.05 ^b	2613 ± 331.92 ^a	86.3	77.29

^a † Water vapor permeability; †† tensile strength; ††† Young's Modulus. ^{a–d} Different superscripts within the same column indicate significant differences among formulations regarding the same property.



type of properties was obtained with respect to UV-light barrier capacity. The presence of GA in the films, regardless of the proportion, increased this barrier more than 70%. The phenolic structure of GA underlies this phenomenon. Thus, GA blocks UV-light almost completely with a small sacrifice of film transparency. Transparency and UV-light blocking capacity are desirable attributes in food packaging films since UV rays promote food oxidation in turn destroying nutrients and bioactive compounds.³⁹

The surface morphology of the films incorporating GA is shown in Fig. 5. An adequate distribution of GA embedded in the matrix surface is observed as small white spots in the form of ovals. These results are in agreement with those presented by Singh *et al.*, who observed the surface morphology of chitosan, sodium carbonate and GA films.⁴¹

Antioxidant properties of gallic acid-loaded polymer films.

The antioxidant activity of films acting as a free radical scavenger is one of the most important properties in active food packaging. Free radicals cause discoloration, rancidity, and off-flavour formation in packaged foods.⁴² This is why films with active ingredients capable of scavenge these radicals are

desirable for optimal performance of the materials. The antioxidant activity of GA-loaded films was measured by two different assays: radical scavenging activity by DPPH method (RSA) and antioxidant power by ABTS method (AOP). There are numerous assays available for the estimation of the antioxidant activity of materials, each having its own specific mechanism for measuring these properties. Therefore, in order to obtain an accurate estimation of the antioxidant activity of the films, two different assays were performed. The results of these tests are shown in Fig. 6.

The blank films (neat CMC, 3% H-MCNF, and 3% V-MCNF) showed no antioxidant activity in any of the tests. Regarding the DPPH test, no significant differences were found between using one type of nanofibres or another as reinforcing agent. However, the dose of GA added to the films was decisive. Thus, those incorporating 5% GA achieved around 25% RSA, while more than 60% RSA was achieved when the GA dose was increased to 10%. The high antioxidant activity achieved with the presence of GA is related to the number and position of free phenolic hydroxyl groups in the molecule. These intercept the free radical chain forming a stable product that does not initiate

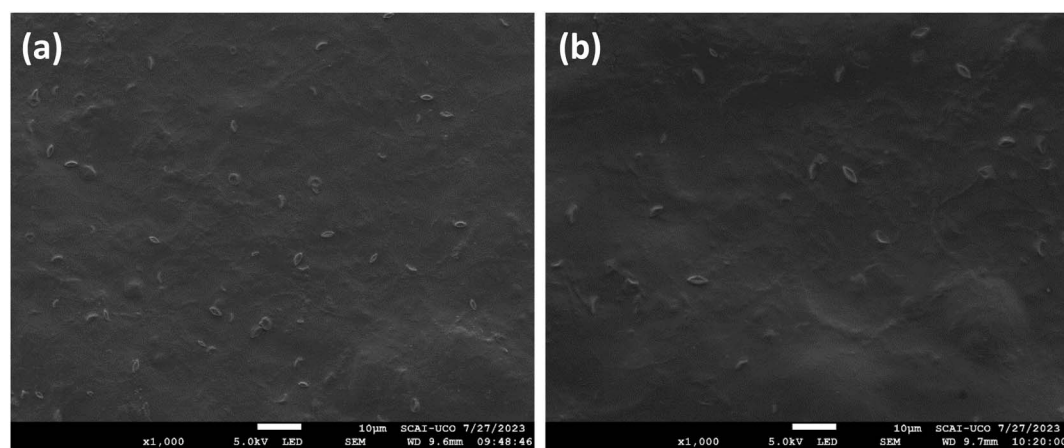


Fig. 5 SEM images of (a) H-10% GA and (b) V-10% GA.



Fig. 6 Antioxidant properties of the bioactive films determined by different tests. (a) and (b) Different letters above the bars indicate significant differences among formulations ($p \leq 0.05$).



or propagate lipid oxidation.²⁰ In the ABTS assay, high AOPs were reported for all films incorporating GA. In this case, no significant differences were found between the proportion of GA added but between the type of nanofibres applied as reinforcement. Thus, H-MCNF films loaded with GA reached almost 100% AOP, while V-MCNF films reached 80%. These differences can be attributed to the lower specific surface area of V-MCNF compared to H-MCNF and leading to less contact of GA with free radicals.

These differences between DPPH and ABTS methods are explained by several factors: (i) GA is more soluble in hydro-alcoholic mixtures such as those used as solvent in the ABTS assay instead of more polar solvents such as methanol used in DPPH and (ii) the polymeric matrix has a low swelling rate in the methanol used in the DPPH assay which results in a lower exposure of the active groups.³⁷ The results obtained by means of the two different assays were similar to those reported in literature for CMC films reinforced with zinc oxide nanoparticles and loaded with grape seed extract or gallic acid as active agents.^{38,43} These results were directly related to a successful use of the films in active red meat packaging applications. The strong antioxidant activity of the GA-loaded films prepared in this study suggests their suitability for use in food active packaging.

Antibacterial properties. The results of the antimicrobial activity of the developed films are shown in Fig. 7. The incorporation of GA in the film formulation conferred bioactive properties to the materials, not being this effect observed for the blank films (3% H-MCNF and 3% V-MCNF). The antimicrobial activity was found to be closely related with the structural nature of the bacteria used in the assay. Of the two different bacteria tested, no inhibition was observed for the Gram-negative *E. coli*. However, the materials showed to inhibit the growth of the Gram-positive *S. aureus*. This resistance exhibit by *E. coli* could be due to the presence of an outer membrane in its cell structure, creating a permeation barrier that protects the bacteria against the irreversible changes caused by GA. However, the absence of this membrane in *S. aureus* makes it more susceptible to antimicrobial substances.⁴⁴



Fig. 7 Antimicrobial properties of the bioactive films against *S. aureus*. (a) and (b) Different letters above the bars indicate significant differences among formulations ($p \leq 0.05$).

Focusing on *S. aureus*, the inhibition values were significantly higher ($p < 0.05$) for the GA-loaded H-MCNF films compared to GA-loaded V-MCNF. The higher lengths observed in V-MCNF, leads to a more entangled structure in which GA remains embedded, hindering its release to the agar.¹⁵ For both types of samples, no significant differences ($p > 0.05$) were observed between the use of 5% and 10% wt.

Conclusions

The reinforcing effect of (ligno)cellulose nanofibres obtained from various agricultural residues (horticultural residues and vine shoots) on CMC films, as well as the joint addition of (L) CNF and GA as an active ingredient for use in active food packaging has been evaluated. The following conclusions are drawn from the present work:

- (1) The incorporation of 3% horticultural-nanofibres and vine shoots-nanofibres allowed achieving a reinforcing effect of up to 381% and 283%, respectively, compared to neat CMC film.
- (2) A moderate improvement of WVP was obtained by including nanofibres in the films with high UV-light blocking capacity.
- (3) Both types of agricultural residues are useful for the production of nanofibres acting as reinforcement in CMC films. After the evaluation of different types of nanofibres and pretreatments applied to obtain them, it was concluded that the optimal candidates were H-MCNF and V-MCNF.
- (4) The addition of GA in the films resulted in an enhancement of all properties: WVP, TS, YM and UV-light blocking capacity improved by 50%, 70%, 94% and 70%, respectively.
- (5) The bioactive films exhibited high antioxidant activity with only 5% GA in their formulation, in addition to excellent antimicrobial power against Gram-positive bacteria.

These results suggested the suitability of cellulose nanofibre-reinforced CMC films from agricultural residues and loaded with GA as an excellent sustainable and bio-based solution for the active food packaging industry.

Author contributions

Conceptualisation, E. R., E. E., and A. R.; methodology, J. D. H.-N., R. M.-M., and E. R.; formal analysis, J. D. H.-N., E. R., and R. M.-M., and E. E.; investigation, E. R., E. E., and A. R.; data curation, E. R., and R. M.-M.; writing—original draft preparation, E. R., and A. R.; writing—review and editing, E. E., and A. R. All authors have read and agreed to the published version of the manuscript.

Conflicts of interest

There are no conflicts to declare.

Acknowledgements

The authors acknowledge the financial support from the Department of Economic Transformation, Industry, Knowledge, and Universities (Regional Government of Andalusia).



This research is part of the project: *Valorización de residuos agrícolas mediante la obtención de productos útiles para la industria agroalimentaria*, P-18-RT-4064. The authors also thank the staff of the Instituto Químico para la Energía y el Medioambiente (IQUEMA) of the Universidad de Córdoba.

References

- European Parliament, *Directive (EU) 2019/904 of the European Parliament and of the Council of 5 June 2019 on the reduction of the impact of certain plastic products on the environment*, 2019.
- K. Eissenberger, A. Ballesteros, R. De Bisschop, E. Bugnicourt, P. Cinelli, M. Defoin, E. Demeyer, S. Fürtauer, C. Gioia, L. Gómez, R. Hornberger, C. Ißbrücker, M. Mennella, H. von Pogrell, L. Rodríguez-Turienzo, A. Romano, A. Rosato, N. Saile, C. Schulz, K. Schwede, L. Sisti, D. Spinelli, M. Sturm, W. Uyttendaele, S. Verstichel and M. Schmid, *Polymers*, 2023, **15**, 1184.
- J. Fernández-Santos, C. Valls, O. Cusola and M. B. Roncero, *Int. J. Biol. Macromol.*, 2022, **211**, 218.
- J. Wang, X. Han, C. Zhang, K. Liu and G. Duan, *Nanomaterials*, 2022, **12**, 3158.
- P. Ezati, Z. Riahi and J.-W. Rhim, *Food Hydrocolloids*, 2022, **122**, 107104.
- H. F. Youssef, M. E. El-Naggar, F. K. Fouda and A. M. Youssef, *Food Packag. Shelf Life*, 2019, **22**, 100378.
- N. Jannatyha, S. Shojaei-Aliabadi, M. Moslehishad and E. Moradi, *Int. J. Biol. Macromol.*, 2020, **164**, 2323.
- Y. Ebrahimi, S. J. Peighambaroust, S. H. Peighambaroust and S. Z. Karkaj, *J. Food Sci.*, 2019, **84**, 2537.
- Y. Chen, M. Hanshe, Z. Sun, Y. Zhou, C. Mei, G. Duan, J. Zheng, E. Shiju and S. Jiang, *Int. J. Biol. Macromol.*, 2022, **207**, 130.
- R. Si, J. Pu, H. Luo, C. Wu and G. Duan, *Polymers*, 2022, **14**, 5479.
- X. Wang, Q. Wang and C. Xu, *Bioengineering*, 2020, **7**, 40.
- E. Rincón, E. Espinosa, M. Pinillos and L. Serrano, *Polymers*, 2023, **15**, 866.
- M. Li, X. Tian, R. Jin and D. Li, *Ind. Crops Prod.*, 2018, **123**, 654.
- E. Espinosa, E. Rincón, R. Morcillo-Martín, L. Rabasco-Vílchez and A. Rodríguez, *Ind. Crops Prod.*, 2022, **187**, 115413.
- J. De Haro-Niza, E. Rincón, Z. Gonzalez, E. Espinosa and A. Rodríguez, *Nanomaterials*, 2022, **12**, 4447.
- P. Ezati and J.-W. Rhim, *ACS Appl. Polym. Mater.*, 2021, **3**, 2131.
- W.-F. Lai, *Int. J. Mol. Sci.*, 2021, **23**, 12.
- E. Rincón, L. Serrano, A. Balu, J. J. Aguilar, R. Luque and A. García, *Materials*, 2019, **12**, 2356.
- K. Szabo, L. Mitrea, L. F. Călinoiu, B.-E. Teleky, G. A. Martău, D. Plamada, M. S. Pascuta, S.-A. Nemeş, R.-A. Varvara and D. C. Vodnar, *Molecules*, 2022, **27**, 7977.
- F. Luzzi, E. Pannucci, L. Santi, J. M. Kenny, L. Torre, R. Bernini and D. Puglia, *Polymers*, 2019, **11**, 1999.
- J. Promsorn and N. Harnkarnsujarit, *Food Control*, 2022, **142**, 109273.
- B. J. Ahn, K. K. Gaikwad and Y. S. Lee, *J. Appl. Polym. Sci.*, 2016, DOI: [10.1002/app.44138](https://doi.org/10.1002/app.44138).
- Z. Fang, D. Lin, R. D. Warner and M. Ha, *Food Chem.*, 2018, **260**, 90.
- A. International, *ASTM E96/E96M-10, Standard Test Methods for Water Vapor Transmission of Materials 2010*, 2010.
- A. International, *ASTM D882-18, Standard Test Method for Tensile Properties of Thin Plastic Sheetings 2018*, 2018.
- E. Rincón, E. Espinosa, M. T. García-Domínguez, A. M. Balu, F. Vilaplana, L. Serrano and A. Jiménez-Quero, *Carbohydr. Polym.*, 2021, **272**, 118477.
- S. Roy and J.-W. Rhim, *Food Hydrocolloids*, 2019, **94**, 391.
- H.-J. Kim, S. Roy and J.-W. Rhim, *J. Environ. Chem. Eng.*, 2021, **9**, 106043.
- S. S. Karkhanis, N. M. Stark, R. C. Sabo and L. M. Matuana, *Composites, Part A*, 2018, **114**, 204.
- M. Ghaderi, M. Mousavi, H. Yousefi and M. Labbafi, *Carbohydr. Polym.*, 2014, **104**, 59.
- E. Espinosa, I. Bascón-Villegas, A. Rosal, F. Pérez-Rodríguez, G. Chinga-Carrasco and A. Rodríguez, *Int. J. Biol. Macromol.*, 2019, **141**, 197.
- M. Zhang, S. Jiang, F. Han, M. Li, N. Wang and L. Liu, *Carbohydr. Polym.*, 2021, **264**, 118033.
- R. Auras, B. Harte and S. Selke, *Macromol. Biosci.*, 2004, **4**, 835.
- S. Shankar, J.-W. Rhim and K. Won, *Int. J. Biol. Macromol.*, 2018, **107**, 1724.
- M. Li, X. Tian, R. Jin and D. Li, *Ind. Crops Prod.*, 2018, **123**, 654.
- S. Arfelis, R. J. Aguado, D. Civancik, P. Fullana-i-Palmer, M. À. Pèlach, Q. Tarrés and M. Delgado-Aguilar, *Sci. Total Environ.*, 2023, **874**, 162482.
- P. Ezati and J.-W. Rhim, *Food Hydrocolloids*, 2020, **102**, 105629.
- S. Yadav, G. K. Mehrotra and P. K. Dutta, *Food Chem.*, 2021, **334**, 127605.
- K. Limpisophon and G. Schleining, *J. Food Sci.*, 2017, **82**, 80.
- X. Sun, Z. Wang, H. Kadouh and K. Zhou, *LWT-Food Sci. Technol.*, 2014, **57**, 83.
- G. Singh, S. Singh, B. Kumar and K. K. Gaikwad, *Journal of Food Measurement and Characterization*, 2021, **15**, 585–593.
- Y. Liu, Y. Qin, R. Bai, X. Zhang, L. Yuan and J. Liu, *Int. J. Biol. Macromol.*, 2019, **134**, 993.
- R. Priyadarshi, S.-M. Kim and J.-W. Rhim, *Sustainable Mater. Technol.*, 2021, **29**, e00325.
- Y. Wang, H. Du, M. Xie, G. Ma, W. Yang, Q. Hu and F. Pei, *Food Packag. Shelf Life*, 2019, **22**, 100401.

